Hypoxia influences polysome distribution of human ribosomal protein S12 and alternative splicing of ribosomal protein mRNAs

ANDREA BRUMWELL, LESLIE FELL, LINDSAY OBRESS, and JAMES UNIACKE

Department of Molecular and Cellular Biology, University of Guelph, Guelph, Ontario N1G 2W1, Canada

ABSTRACT

Ribosomes were once considered static in their composition because of their essential role in protein synthesis and kingdom-wide conservation. The existence of tolerated mutations in select ribosomal proteins (RPs), such as in Diamond-Blackfan anemia, is evidence that not all ribosome components are essential. Heterogeneity in the protein composition of eukaryotic ribosomes is an emerging concept with evidence that different pools of ribosomes exist with transcript-specificity. Here, we show that the polysome association of ribosomal proteins is altered by low oxygen (hypoxia), a feature of the tumor microenvironment, in human cells. We quantified ribosomal protein abundance in actively translating polysomes of normoxic and hypoxic HEK293 cells by tandem mass tags mass spectrometry. Our data suggest that RPS12 (eS12) is enriched in hypoxic monosomes, which increases the heavy polysome association of structured transcripts APAF-1 and XIAP. Furthermore, hypoxia induced five alternative splicing events within a subset of RP mRNAs in cell lines. One of these events in RPS24 (eS24 protein) alters the coding sequence to produce two protein isoforms that can incorporate into ribosomes. This splicing event is greatly induced in spheroids and correlates with tumor hypoxia in human prostate cancer. Our data suggest that hypoxia may influence the composition of the human ribosome through changes in RP incorporation and the production of hypoxia-specific RP isoforms.

Keywords: hypoxia; ribosome; splicing; cancer

INTRODUCTION

The perception of the ribosome, the nexus of protein synthesis within the cell, has changed dramatically throughout the past couple of decades. No longer viewed as a completely rigid and passive structure, mounting evidence suggests that cells maintain a heterogeneous pool of ribosomes. Altered stoichiometry of ribosomal proteins (RPs) has been observed in both ribosomes of wild-type yeast and mouse embryonic stem cells (Slavov et al. 2015; Shi et al. 2017). Further, the presence of certain RPs in ribosomes may specify transcript selection. Two proteins identified as substoichiometric in mouse embryonic stem cells, RPL10A and RPS25, bind different categories of mRNAs when present in ribosomes, such as those involved in extracellular matrix organization and the vitamin B_{12} pathway, respectively (Shi et al. 2017). The recent use of advanced mass spectrometric techniques to measure ribosome stoichiometry identified minimal heterogeneity in wild-type human 40S subunits, albeit RPS25 was again identified as substoichiometric (van de Waterbeemd et al. 2018). Minimal heterogeneity in ribosome composition is unsurprising in unstressed cells, but it is tempting to speculate that stressors or other environmental stimuli may alter gene expression through changes in RP incorporation into the ribosome.

In response to environmental insults such as heat shock, nutrient deprivation, or hypoxia, cells mount an adaptive stress response often through the regulation of translation. Protein synthesis is suppressed during stress, but the translation initiation of select transcripts is regulated to aid in cell survival, preventing DNA damage, and recovery (Liu and Qian 2014). Processes to maintain this selective translation can include cap-independent initiation through internal ribosome entry sites (IRES) or cap-independent translation enhancers, upstream open reading frames, noncanonical cap-dependent initiation via cap-binding homolog eIF4E2, and the use of alternative

Corresponding author: juniacke@uoguelph.ca

Article is online at http://www.rnajournal.org/cgi/doi/10.1261/rna.070318.119.

initiation factors such as eIF4G3, DAP5, and eIF5B (Holcik and Sonenberg 2005; Uniacke et al. 2012; Ho et al. 2016, 2018; Lacerda et al. 2017; Bryant et al. 2018).

Indeed, ribosome regulation during stress is not a novel concept. Actively translating ribosomes from nutrient-deprived *Escherichia coli* are enriched with rRNA encoded by a specific rDNA operon. Nine out of ten variant nucleotides of this rDNA operon are located in the beak region of the ribosome, and these ten variant nucleotides are sufficient to alter the expression and translation of genes associated with nutrient stress (Kurylo et al. 2018). Exposure of yeast to high salt and high pH stress induces RPS26-deficient ribosomes that preferentially translate mRNAs bearing Kozak sequence variations (Ferretti et al. 2017). Similar to RPS26, the presence of RPL38 and RPL13A in ribosomes also affects the ability of ribosomes to translate IRES-containing transcripts while having no effect on cap-dependent translation initiation (Chaudhuri et al. 2007; Kondrashov et al. 2011; Xue et al. 2015).

Despite amassing evidence of ribosome heterogeneity in wild-type cells, or in stressed *E. coli* and yeast, the regulation of RPs in human ribosomes under environmental stimuli or stress has yet to be studied. Given the relevance of hypoxia in human physiology and disease, namely embryonic development and tumor biology (Semenza 2012), we investigated the influence of hypoxia (1% O_2) on the regulation of human RPs and their incorporation into ribosomes. We first used tandem mass tags (TMT) mass spectrometry to quantify alterations in polysome-associated RPs between hypoxic and normoxic HEK293 cells. We identified RPS12 (eS12) as having an increased monosome to polysome ratio in hypoxia relative to normoxia. The exogenous enrichment of RPS12 in monosomes leads to enhanced heavy polysome association of APAF-1 and XIAP mRNAs. We next examined alternative splicing events (ASEs) in RP mRNAs that could lead to hypoxia-induced RP isoforms. An analysis of 68 ASEs in RP mRNAs revealed five events that were induced by hypoxia in HEK293. Of these five events, an exon inclusion event in RPS24 was consistently increased in spheroids (3D hypoxic cell culture models) of four cell lines, and displayed a significant weak correlation with hypoxia in human prostate tumor samples. Our data suggest that hypoxia produces changes in polysome association of select RPs and alters the ratio of select RP mRNA splice variants.

RESULTS

Hypoxia influences the participation of select RPs in actively translating ribosomes of HEK293 cells

To investigate the effects of hypoxia on polysome association of RPs, we cultured HEK293 cells in normoxia (21% O_2) or hypoxia (1% O_2) for 24 h. We isolated 80S monosomes (M; single ribosomes), light polysomes (L; 2–4 ribosomes/transcript), and heavy polysomes (H; ≥ 5 ribosomes/transcript) via sucrose density gradient fractionation of an equal number of cells (Fig. 1A). M, L, and H fractions in both normoxia and hypoxia were tagged with separate isobaric labels for a single injection for TMT mass spectrometry. Among the 3232 unique proteins identified across three biological replicates, we detected 78 of the 80 canonical RPs and three paralogs with an average of 11 unique peptides. RPL39 (or the unified nomenclature eL39) and RPL41 (eL41) were not detected perhaps due to small size (see Supplemental Material source data file for Fig. 1). We calculated abundance ratios of RPs in L and H fractions relative to M, obtaining L/M and H/M ratios in normoxia and hypoxia (Fig. 1B). The M fraction was used as reference within each condition to control for oxygen-dependent differences in ribosome biogenesis, ribophagy, and translation capacity. In accordance with a higher ribosome density in the polysome fractions, most RPs are more abundant in L and H relative to M (positive $\log_2$ fold change; Fig. 1B). In normoxia, 68/81 and 81/81 RPs displayed L/M and H/M ratios ≥1, respectively (Fig. 1B). Similarly, 50/81 and 80/81 RPs displayed hypoxic L/M and H/M ratios ≥1, respectively (Fig. 1B). To highlight hypoxia-specific changes in RP polysome association, we divided hypoxic L/M or H/M by normoxic L/M or H/M (Fig. 1C). Since hypoxia reduces global translation (Liu and Simon 2004), it was not surprising that most RPs were less associated with polysomes in hypoxia compared to normoxia (Fig. 1C). Indeed, 56/81 and 68/81 ratios had a negative $\log_2$ fold change (Fig. 1C). Interestingly, from the RPs that had a positive $\log_2$ fold change, only three (RPL7L1, RPL8 [uL2], and RPL27A [uL15]) significantly increased by >20% in hypoxic L/M or H/M relative to normoxia (solid bars; Fig. 1C). RPS12 (eS12) was the only RP to be more abundant in M relative to H in hypoxia (H/M < 1), and was also more abundant in hypoxic M relative to L (Fig. 1B). Furthermore, RPS12 decreased 2.2-fold in hypoxic relative to normoxic H/M (Fig. 1C), as confirmed by western blot (Supplemental Fig. S1A,B). A western blot on individual fractions of a whole polysome gradient shows that RPS12 is enriched in hypoxic monosomes (Supplemental Fig. S1C). The antibody against RPS12 recognizes its carboxy-terminal region, indicating that changes in abundance were not due to nascent polypeptides. These data suggest that within a heterogeneous pool of ribosomes, RPL7L1, RPL8, and RPL27A are more likely whereas RPS12 is less likely to be incorporated into hypoxic polysomes.

RPS12 overexpression increases heavy polysome association of APAF-1 and XIAP mRNAs

While the mass spectrometry data indicated a reduction of RPS12 in hypoxic heavy polysomes relative to normoxia, there was also an enrichment of RPS12 in monosomes (Fig. 1). Indeed, when validated via western blot, the

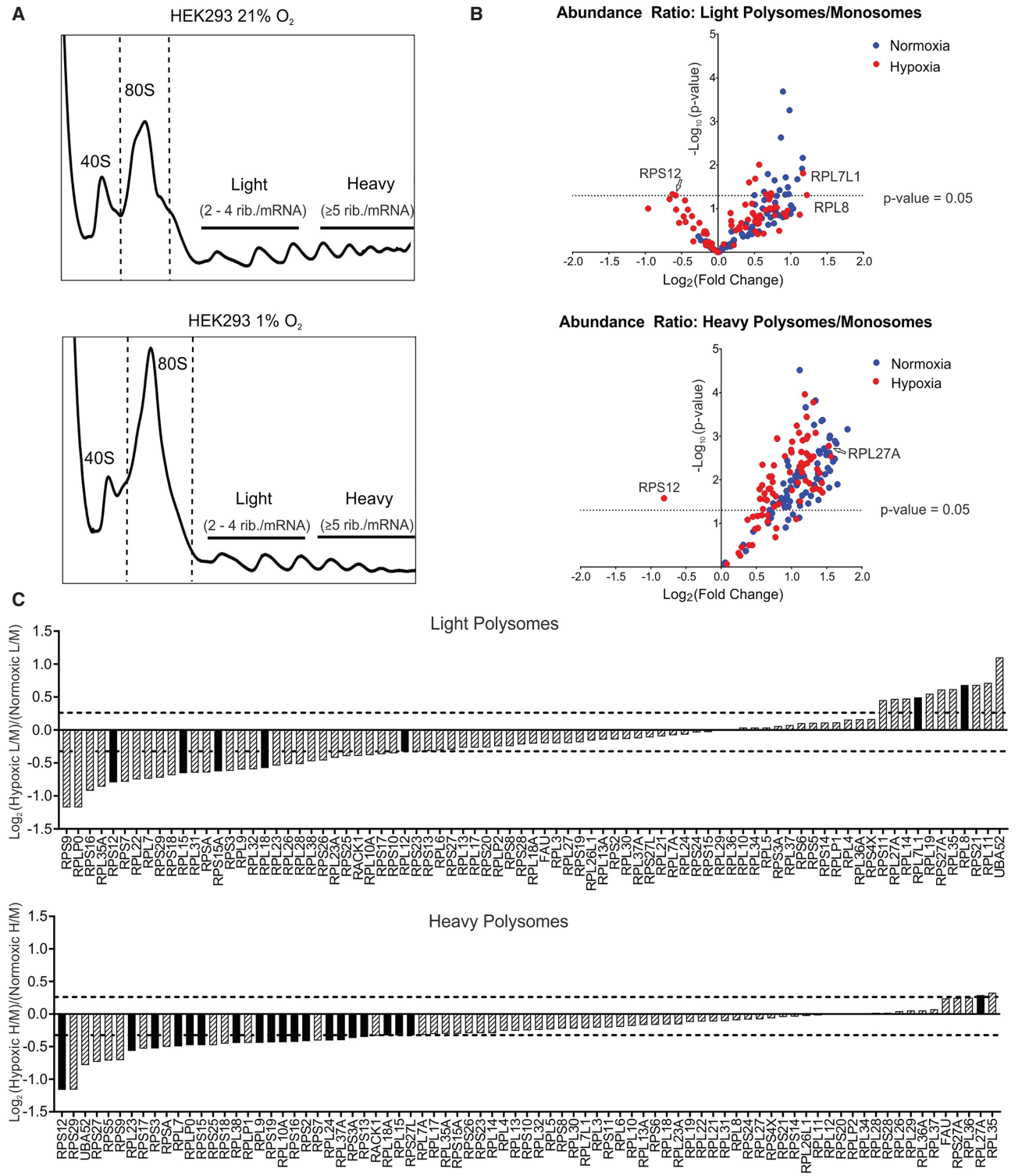

FIGURE 1. The abundance of four ribosomal proteins is altered in hypoxic relative to normoxic polysomes. (*A*) Fractionated ultracentrifuged cell lysates from HEK293 in 21% O_2 (normoxia) and 1% O_2 (hypoxia) were pooled into 80S monosomes (M; within dotted line), light polysomes (L), and heavy polysomes (H). (*B*) Volcano plot of the abundance ratio using the mean abundances from three biological replicates to calculate the L/M and H/M ratios. Dotted line represents $P = 0.05$ using two-tailed unpaired *t*-test. (*C*) The ratio of hypoxic L/M or H/M to normoxic L/M or H/M was calculated and represented as $\log_2$ fold change. Dashed line represents cut-off value of ±0.2 non-$\log_2$ transformed change in hypoxic L/M or H/M relative to normoxic (L/M or H/M). Solid bars represent proteins above this cut-off that were statistically significant in hypoxic polysomes relative to monosomes. See Supplemental Material source data file for Figure 1.

enrichment of RPS12 in hypoxic monosomes was more evident than its reduction in heavy polysomes (Supplemental Fig. S1). Structural studies place RPS12 in the beak of the ribosome where it interacts with DHX29 (Hashem et al. 2013). Since DHX29 has been linked to the translation initiation of structured transcripts (Parsyan et al. 2009; Pisareva and Pisarev 2016), we investigated whether RPS12 had a similar role. Because siRNA-mediated depletion of most RPs leads to impaired ribosome biogenesis (Robledo et al. 2008; O'Donohue et al. 2010), we explored RPS12 overexpression. Since exogenous carboxyl terminal myc-tagged RPS12 enriched specifically in monosomes and light polysomes (Supplemental Fig. S2), this provided a condition that exaggerated the hypoxic phenotype. Indeed, APAF-1 mRNA, a transcript with a very highly structured (ΔG −289.1 kcal/mol via mfold) and long (587 nt) 5′ UTR, associated significantly more with hypoxic heavy polysomes in RPS12 overexpressing cells relative to the empty vector control (Fig. 2A). We also tested XIAP mRNA, a DHX29-dependent transcript (Parsyan et al. 2009) with a moderately structured (ΔG −65.0 kcal/mol) and shorter (159 nt) 5′ UTR, which associated more with hypoxic heavy polysomes in RPS12 overexpressing cells albeit less so than APAF-1 (Fig. 2A). GAPDH and β-Actin mRNAs, two transcripts with short 5′ UTRs (<100 nt) with weak secondary structures, displayed no change in their polysome association between RPS12 overexpressing cells and controls (Fig. 2A). Overexpression of RPS12 does not appear to alter global translation (Supplemental Fig. S2). Crystal structures of the ribosome indicate that the carboxyl terminus of RPS12 is solvent-exposed (Anger et al. 2013), so the tag should not interfere with ribosome

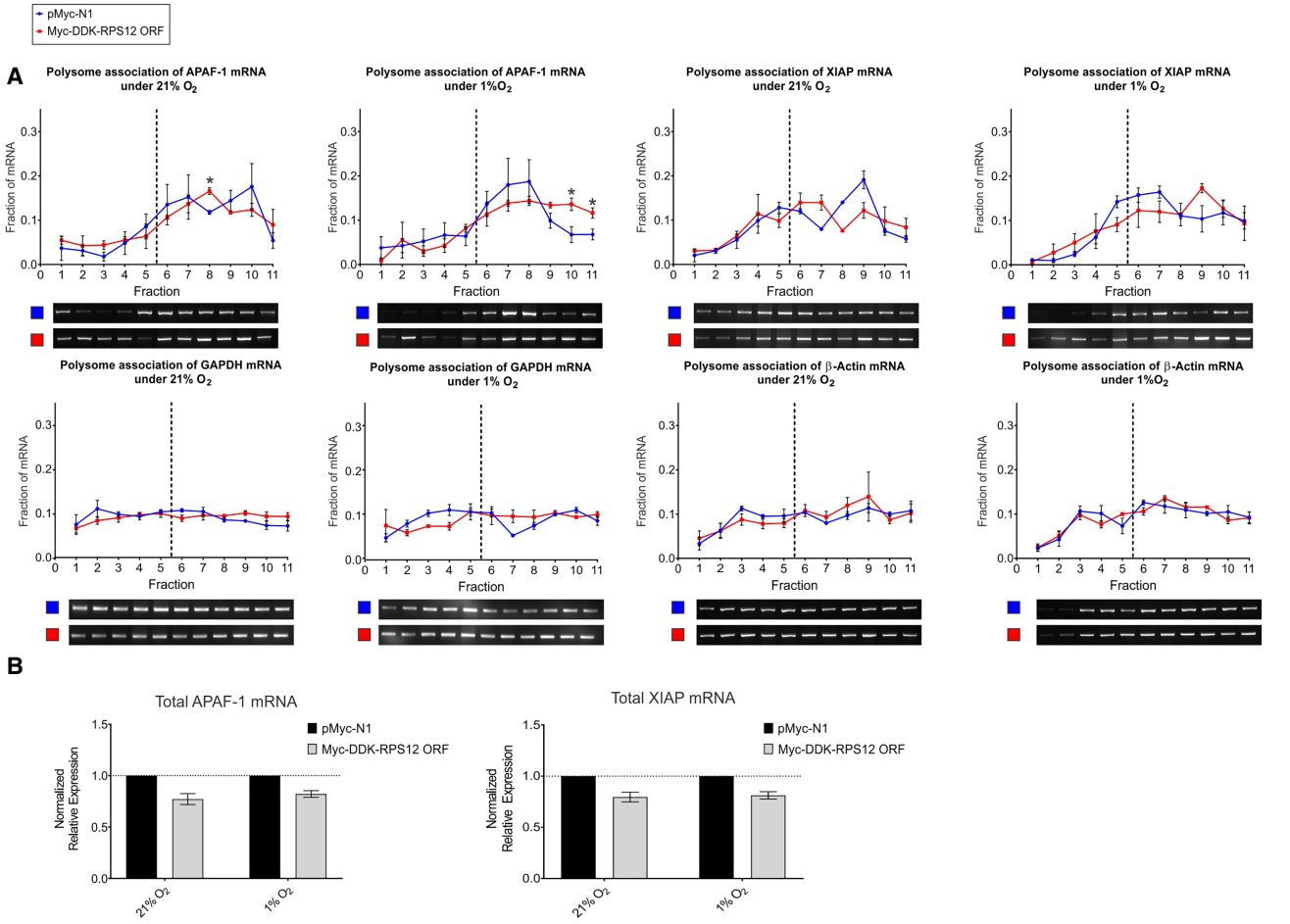

FIGURE 2. RPS12 overexpression affects heavy polysome association of APAF-1 and XIAP mRNAs. (*A*) Semi-quantitative RT-PCR was used to measure the abundance of APAF-1, XIAP, GAPDH, and β-Actin mRNAs in polysome fractions of normoxic (21% O_2) and hypoxic (1% O_2) HEK293 cells overexpressing RPS12 (eS12) with the Myc-DDK-RPS12 ORF vector (red line) or control cells expressing the empty vector pMyc-N1 (blue line). The fraction of mRNA in each lane was calculated based on total band intensity of the transcript across the entire polysome gradient. Dashed line denotes the start of the polysome fractions. A representative image is shown. (*B*) Total levels of APAF-1 and XIAP mRNA were measured in normoxic and hypoxic HEK293 control cells and those overexpressing RPS12 using RT-qPCR. The $\Delta\Delta C_t$ method was used, normalizing to reference gene *RPL13A*, and fold-change made relative to empty vector control. Data ($n = 3$), mean ± SEM. Two-tailed unpaired *t*-tests were performed.

incorporation and indeed exogenous RPS12 associated with the polysome fractions to a similar degree as the endogenous RP (Supplemental Fig. S2). However, a portion of exogenous RPS12 associated with the free fraction (fraction 1; Supplemental Fig. S2). Some free-floating RPs can stabilize p53 (Zhang and Lu 2009), which induces APAF-1 transcription (Robles et al. 2001). We show that p53 (Supplemental Fig. S3) and total APAF-1 mRNA levels (Fig. 2B) do not change between RPS12 overexpressing and control cells. Given that total APAF-1 and XIAP mRNA levels do not increase in RPS12 overexpressing cells (Fig. 2B), this suggests that the increase in monosome and light polysome-associated RPS12 observed in hypoxia contributes to the higher translation efficiency of these structured transcripts. Of note, normoxic overexpression of RPS12 did not increase the translation efficiency of APAF-1 and XIAP mRNAs suggesting that other hypoxia-induced factors could be required.

Hypoxia induces alternative splicing events in ribosomal protein mRNAs in HEK293

Another way that hypoxia could influence ribosome composition is through the generation of RP isoforms via hypoxia-regulated alternative splicing events (ASEs). We examined a panel of 68 ASEs in RP transcripts in normoxic and hypoxic HEK293 cells by end-point PCR. Primer pairs flanking specific ASEs produced long amplicons that included a certain exon or short amplicons that either excluded the exon or included an alternative shorter exon (Supplemental Table S1). The expression ratio of the long amplicon (L) relative to the short (S) was quantified by capillary electrophoresis and expressed as percent splicing index [PSI; $L/(S+L) \times 100$]. Hypoxia was confirmed by measuring the expression of *SLC2A1*/GLUT1 mRNA (Supplemental Fig. S4). Only 6/68 ASEs displayed ≥10% PSI difference between normoxia and hypoxia (ΔPSI), while the majority (40/68) of ASEs had 0% ΔPSI (Fig. 3). A ΔPSI of ≥10% has been previously used as a threshold for validation (Klinck et al. 2008). Of the six ASEs that displayed a ΔPSI of ≥10%, we chose to investigate five events: RPL10e1, RPL17e2, RPL22L1, RPS24e2, and RPS9e3, eliminating RPLP0 due to low detection. These five events can be described as follows: (i) An ASE in RPL10 displayed a complete shift toward inclusion of an alternate 163 bp exon where the PSI increased from 76.1% in normoxia to 100% in hypoxia; (ii) An ASE in RPL17 displayed a reduction in the inclusion of a 17 bp-longer alternative first exon from 40% in normoxia to 26.2% in hypoxia; (iii) the ASE in RPL22L1 displayed a shift toward inclusion of a 67 bp-longer alternative third exon where the PSI increased from 15.7% in normoxia to 30.8% in hypoxia; (iv) An ASE in RPS24 displayed a shift toward inclusion of a 22 bp cassette exon where the PSI increased from 42.3% in normoxia to 56.5% in hypoxia; (v) An ASE in RPS9 displayed

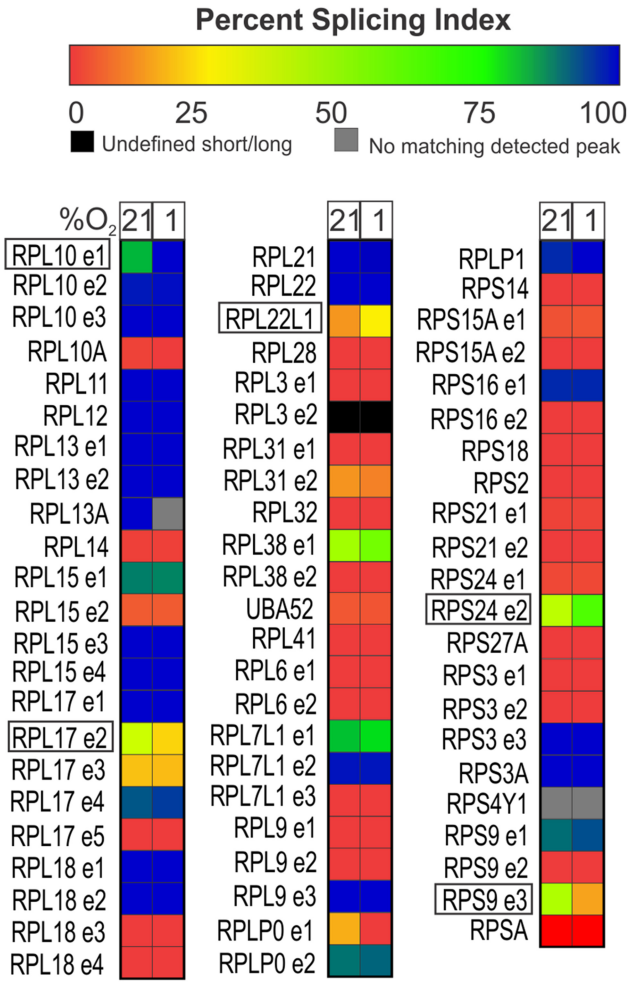

FIGURE 3. Alternative splicing events in five ribosomal protein mRNAs are induced by hypoxia in HEK293 cells. A heat map representing the percent splicing index (PSI; long variant/[short + long variants] × 100) for 68 alternative splicing events (ASEs) in HEK293. Five ASEs (boxed) had a ΔPSI (|hypoxic PSI − normoxic PSI|) ≥ 10%. Nineteen ASEs had a ΔPSI < 10%, 40 had a ΔPSI = 0%, and the ΔPSI was unable to be calculated for three ASEs due to lack of detection or undefined short/long variant. See Supplemental Material source data file for Figure 3.

a shift toward exclusion of a 1372 bp exon rather than three shorter exons where the PSI decreased from 43.8% in normoxia to 17.9% in hypoxia (Supplemental Fig. S5). These data demonstrate that hypoxia has minimal influence on AS in RP mRNAs in HEK293, but that the affected genes could be part of a hypoxia splicing signature.

Hypoxia induces alternative splicing events in ribosomal protein mRNAs in cancer cells

We next investigated whether the hypoxia-induced ASEs in HEK293 RP mRNAs are conserved in other cells lines. We chose three cancer cell lines (U87MG glioblastoma, HCT116 colorectal carcinoma, and PC3 prostate carcinoma) due to the relevance of hypoxia in cancer and tumor

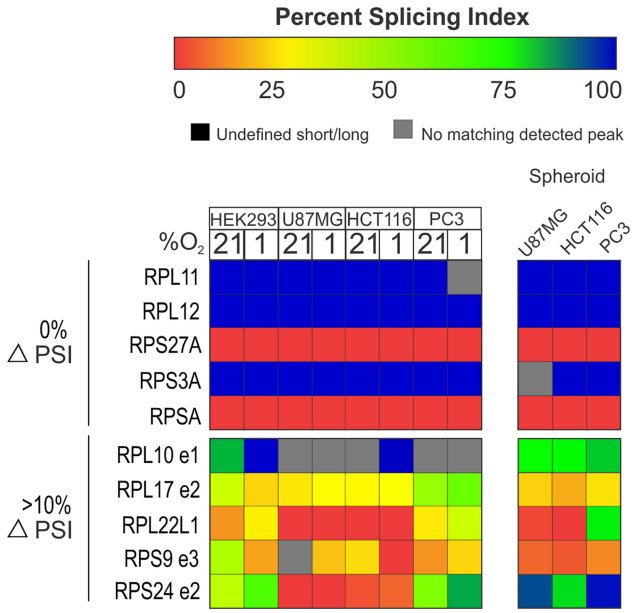

FIGURE 4. Alternative splicing events within ribosomal protein mRNAs were measured in cancer cell lines and their spheroids. Ten alternative splicing events were chosen based on ΔPSI values from Figure 3 of HEK293 cells: Five ASEs with ΔPSI = 0% and five ASEs with ΔPSI ≥ 10% were measured in three cancer cell lines in 21% O_2, 1% O_2, and spheroids. See Supplemental Material source data file for Figure 4.

biology. In addition to cell monolayers, we measured these ASEs in spheroids, avascular models of tumor hypoxia, to identify possible hypoxic tumor biomarkers. Hypoxia was confirmed by *SLC2A1*/GLUT1 mRNA expression in both the monolayers and spheroids (Supplemental Fig. S4).

From the data in HEK293 (Fig. 3), we selected five ASEs that did not change (0% ΔPSI) between normoxia and hypoxia and the five that had a ΔPSI ≥ 10% to determine their reproducibility in the cancer cell lines. Among the ASEs that displayed 0% ΔPSI in HEK293, the PSI were also unchanged in all three cancer cell lines, regardless of oxygen, although the ASE in RPL11 could not be detected in hypoxic PC3 cells (Fig. 4). Overall, the splicing events that changed by >10% in HEK293 displayed some variability across the cancer cell lines, but some commonalities were identified. The amplicons for RPL10e1 were often below the detection threshold of 5 nM, likely due to this ASE not being in the canonical RPL10 mRNAs and thereby making this a poor candidate biomarker. As in hypoxic HEK293, the PSI of RPS9e3 was decreased in hypoxic HCT116, as well as both U87MG and HCT116 spheroids, although the PSI in PC3 cells did not follow this trend. The splicing event in RPL22L1 was reproduced only in PC3 cells where, as with HEK293, the PSI increased in hypoxia and then increased even further in spheroids. Splicing of RPL17e2 had the same trend in all three cancer cell lines, where the PSI decreased in spheroids but increased slightly in hypoxia, unlike HEK293 where the PSI decreased in hypoxia. Similar to RPL22L1, RPS24e2 had an increase in PSI in only hypoxic PC3 cells (as HEK293), but had a dramatic shift toward exon inclusion in spheroids of all three cancer cell lines, increasing by 48%–90% PSI compared to normoxia. Based on these data, we chose the ASE in RPS24 as a candidate marker of hypoxia and/or other features of the spheroid microenvironment. Further, the ASE in RPS24 is the only event that corresponds to the canonical, curated transcripts (NCBI RefSeq) while also affecting the coding sequence. Indeed, we show that the short and long mRNA variants generated by this ASE are translated and produce RP isoforms (eS24) that associate with polysomes (Fig. 5).

Validation of RPS24 AS using RT-qPCR

We next sought to validate the ASPCR spheroid data (Fig. 4) using variant-specific primers and quantitative PCR in hypoxia and spheroids of all four cell lines (Fig. 6). The

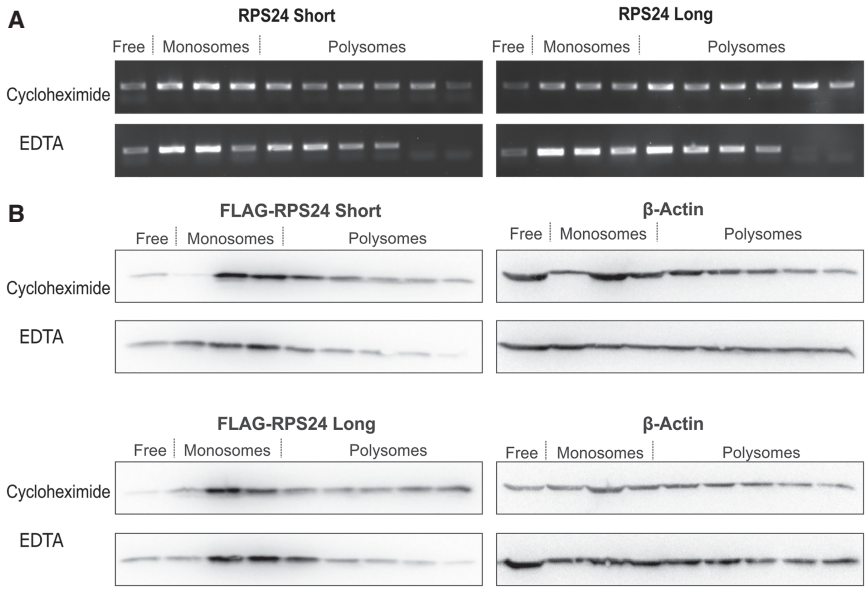

FIGURE 5. Endogenous RPS24 short and long transcript variants, and exogenous protein isoforms associate with polysomes. (*A*) Using transcript variant-specific RPS24 primers, short and long variants were amplified via RT-PCR from polysome fractions with either cycloheximide, or EDTA as a control to dissociate polysomes. (*B*) Polysomes were isolated from two cell lines each stably expressing one of the FLAG-tagged RPS24 protein isoforms (eS24) using cycloheximide and EDTA. Western blots were performed using anti-FLAG, or β-Actin as a control protein not associated with polysomes. Experiments performed in U87MG glioblastoma in normoxia (21% O_2). See Supplemental Table S1 for primer sequences.

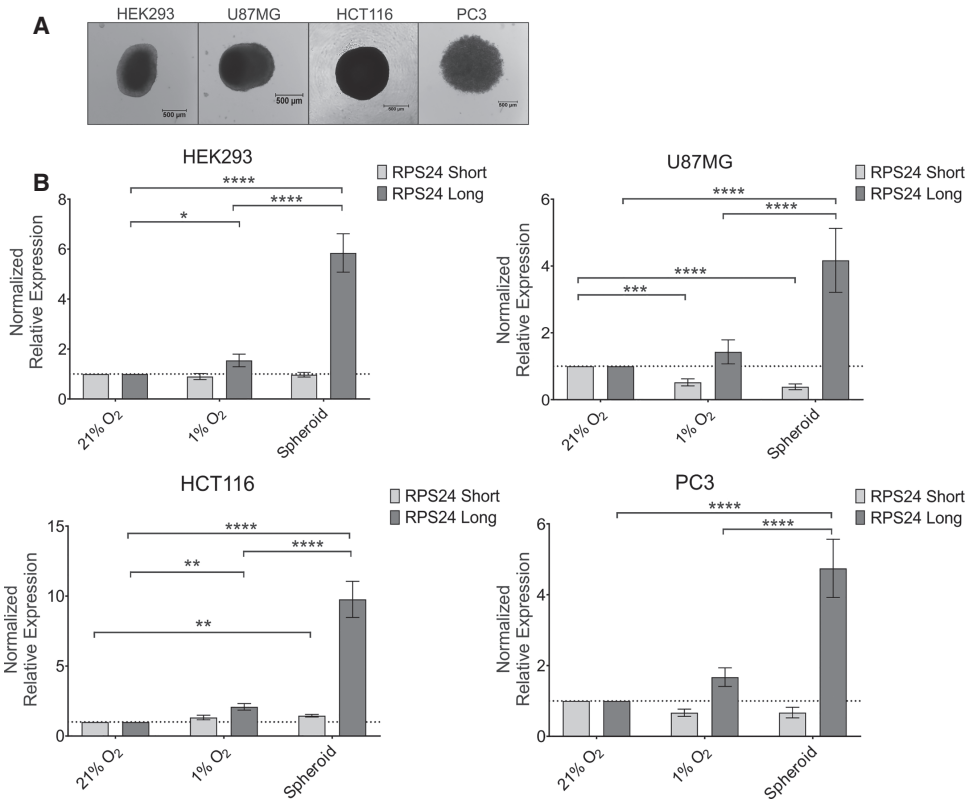

FIGURE 6. The long variant of RPS24 is significantly up-regulated in spheroids of four cell lines. (*A*) Spheroids from four cell lines were imaged and harvested 5 d following cell seeding. (*B*) RT-qPCR using variant-specific RPS24 primers were used to confirm the ASPCR data from Figure 4. The $\Delta\Delta C_t$ method was used, normalizing to reference genes *RPLP0* and *RPL13A*, and the fold-change made relative to normoxia. Data ($n = 8$), mean fold-change ± SEM. One-way ANOVA was performed on the ΔC_t values. (*) $P < 0.05$, (**) $P < 0.01$, (***) $P < 0.001$, (****) $P < 0.0001$. Scale bar, 500 µm.

long variant of RPS24 containing a 22 bp cassette exon increased by 1.4- to 2.1-fold in hypoxic samples of all cell lines. Consistent with the ASPCR data (Fig. 4), the long variant of RPS24 increased greater than or equal to fourfold in spheroids of all cell lines (Fig. 6B). Of note, the short variant of RPS24 decreased in hypoxia relative to normoxia in U87MG and PC3 monolayers and spheroids, further increasing the ratio of long to short RPS24 variants. Therefore, the RPS24 long/RPS24 short variant ratio could be a better predictor of hypoxia and/or the tumor microenvironment than the induction of the RPS24 long variant alone.

Exon inclusion within RPS24 correlates with hypoxia in prostate tumors

We measured the alternative splicing of RPS24 in 96 cDNA samples from prostate tumors or normal tissue. In total: 17 normal samples, 40 Stage II, 30 Stage III, 4 Stage IV, and 5 Stage Not Reported. The degree of hypoxia was determined by measuring carbonic anhydrase-9 (CAIX) expression (Fig. 7A). For RPS24, a less abundant extra-long (XL) amplicon (includes not only the 22 bp cassette exon but also an 18 bp cassette exon) that was detected in HEK293 (Supplemental Fig. S5) was a major amplicon in the tumor samples. Therefore, we calculated two PSI: L/S + L and XL/L + XL. There was a significant weak negative correlation between the CAIX C_t value and both PSI (Fig. 7A). This suggests that hypoxia favors exon inclusion as the more hypoxic samples (i.e., Lower CAIX C_t) had higher PSI values. Conversely, both PSI significantly decreased with cancer stage suggesting that exon exclusion is favored (Fig. 7B), which corresponds with other reports (Danan-Gotthold et al. 2015; Zhang et al. 2015; Munkley et al. 2019). Hypoxia does not always correlate with stage (Hockel et al. 1996), and indeed 13/17 of the hypoxic samples (i.e., $C_t < 31$) were from stage II tumors. Therefore, it was not surprising that the exon inclusion we observed in hypoxia was not more common at later cancer stages. Therefore, our data suggest that RPS24 alternative splicing has the potential to be a marker of tumor hypoxia.

DISCUSSION

Recent studies have highlighted that eukaryotic ribosomes are amenable to alterations in their RP composition, and

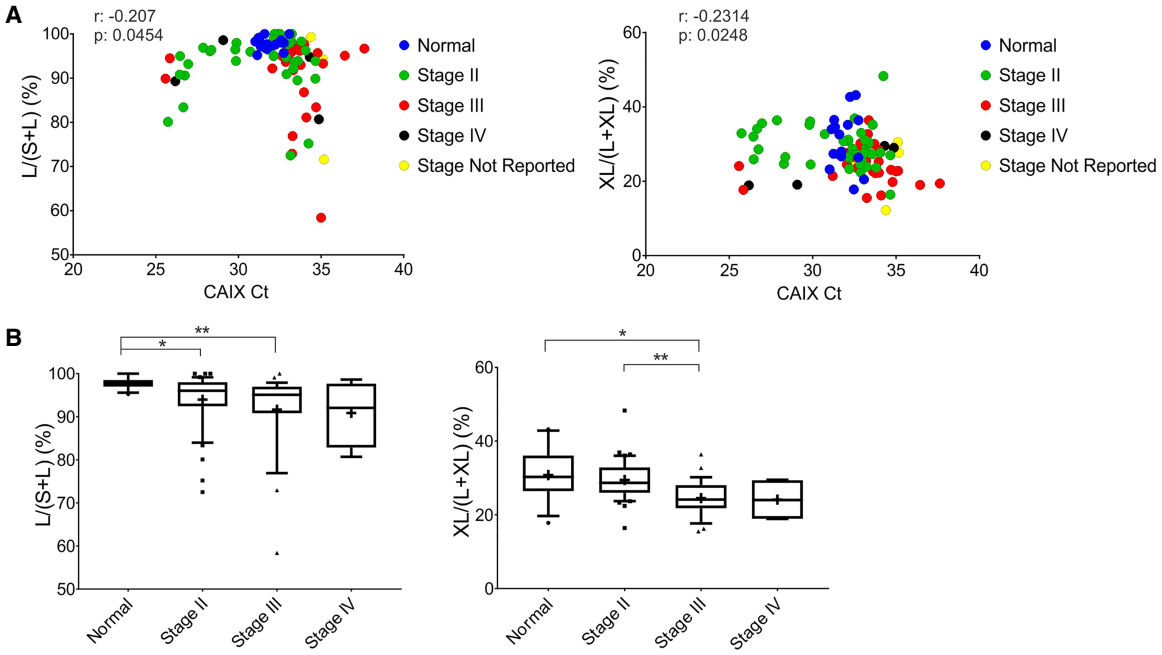

FIGURE 7. The inclusion of an alternative exon in RPS24 is significantly weakly correlated with hypoxia in human prostate tumors. (*A*) An alternative splicing event in RPS24 produces three amplicons in human prostate normal and tumor cDNA samples: short (S), long (L), and extra-long (XL). Because the extra-long amplicon was more abundant than in the cell lines (Supplemental Fig. S5), two PSI were calculated (L/S + L and XL/L + XL) each reflecting the inclusion of a single exon. Each PSI was correlated with the C_t (cycles to threshold in PCR) value of the hypoxia marker CAIX. The Spearman's correlation coefficient (*r*) and associated *P*-value is shown for 94 samples: normal tissue ($n = 16$), stage II ($n = 40$), stage III ($n = 29$), stage IV ($n = 4$), cancer stage not reported ($n = 5$). (*B*) Box plots compare PSI with tumor stage using one-way ANOVA (Kruskal–Wallis) with Dunn's multiple comparisons test. (+) represents mean. (*) $P < 0.05$, (**) $P < 0.01$. See Supplemental Material source data file for Figure 7.

that RPs may play specialized roles in transcript selection (Chaudhuri et al. 2007; Slavov et al. 2015; Ferretti et al. 2017; Shi et al. 2017). Since the function of many RPs is unclear in humans, it is possible that some could regulate ribosome specificity to alter gene expression in response to various stimuli. Hypoxia is implicated in embryonic development, adaptation to altitude, muscle exercise, but also the pathology of cancer, stroke, and heart disease (Semenza 2012). Hypoxia is defined as reduced (≤1% O_2) oxygen availability to cells and is a feature of the tumor microenvironment that drives metastasis and resistance to chemotherapeutics (Semenza 2012). In support of ribosome heterogeneity in cancer, translational control in general has been extensively shown to be deregulated in cancer and is currently a major target of chemotherapeutics (Bhat et al. 2015). Translation regulation has become fertile ground to understanding hypoxic gene expression. Here we show that hypoxia influences polysome association of RPS12 and the alternative splicing of RPS24.

We show that RPS12 is enriched in hypoxic monosomes relative to normoxia, suggesting that this RP may be involved in regulation of hypoxic translation initiation (Coudert et al. 2014). RPS12 is located on the outer surface in the beak of the ribosome, near the mRNA entry channel (Rabl et al. 2011; Khatter et al. 2015) and where translation initiation factors eIF3 and DHX29 bind to cooperate in scanning of structured mRNAs (Pisareva and Pisarev 2016). Overexpression of RPS12 in monosomes caused a greater association of APAF-1 and XIAP mRNAs with hypoxic heavy polysome fractions relative to control. RPS12 overexpression in monosomes minimally influenced the polysome distribution of these mRNAs in normoxia, suggesting a requirement for other hypoxia-induced pathways. APAF-1 mRNA has a long, highly structured 5′ UTR that allows its translation to be cap-independent, highly eIF4A-dependent, and resistant to mTOR suppression (Lyabin and Ovchinnikov 2016). An IRES has been identified in the 5′ UTR of APAF-1 (Coldwell et al. 2000), however 5′ end-dependent scanning has also been shown to occur independent of the IRES (Andreev et al. 2012). Notably, proximity proteomics places RPS12 near eIF4A1 (a helicase that unwinds the 5′ UTR during scanning), suggesting that RPS12 is more frequent in initiating ribosomes (Padrón et al. 2019). We observed a lesser increase, only in hypoxia, of XIAP mRNA association with heavy polysomes when RPS12 was overexpressed in monosomes. This lesser increase could be due to degree of structure within the transcripts, since according to the curated mRNA variants (NCBI), the 5′ UTR of XIAP is less structured than APAF-1. Even though APAF-1 (apoptosis) and XIAP (survival) play opposing roles in the cell, they both contain an IRES which maintains translation efficiency in hypoxia (Holcik

and Sonenberg 2005). Therefore, it is not surprising that both are translated in hypoxia and this could be part of a tug-of-war between cell survival and death under stress. Our data suggest that RPS12 is enriched in hypoxic monosomes to increase the translation efficiency of select transcripts. These transcripts could be selected based on the degree of structure within their 5′ UTR, although future work will be required to fully understand how hypoxic initiating ribosomes select these transcripts via ribosome-associated factors and/or additional features within mRNAs.

It was not surprising that most (63/68) ASEs examined in RP mRNAs were conserved between normoxia and hypoxia due to the important role of the ribosome. Although other splice events could alter RP levels, such as RPL22L1 where the long variant is a predicted target of nonsense-mediated decay, we chose to focus on RPS24 since it alters the coding sequence. Our data suggest that alternative splicing of RPS24 is influenced by hypoxia, but to a greater degree by a combination of factors within spheroids. The longer splice variant of RPS24 produces a protein shortened by three amino acids at the carboxyl terminus (Gupta and Warner 2014). We show that both endogenous RPS24 splice variants are actively translated, and FLAG-tagged versions of the protein isoforms incorporate into polysomes. RPS24 isoforms could produce specialized hypoxic ribosomes through the recruitment of different ribosome-associated proteins since the carboxyl terminus is accessible at the surface. Since the shortened carboxyl terminus produced by the long RPS24 splice variant loses a lysine residue, the two protein isoforms could contain different post-translational modifications that could modulate their activity and/or stability (Khatter et al. 2015). Additionally, proximity proteomics of eIF4A1 showed enrichment of RPS24, highlighting its position near the mRNA entry channel and potential importance in translation initiation (Padrón et al. 2019).

Inclusion of the 22 bp cassette exon or both the 18 and 22 bp cassette exons within RPS24 mRNA had a significant weak positive association with hypoxia in prostate tumors (Fig. 6A), which was consistent with the cell lines where exon inclusion was mildly augmented by hypoxia alone. Conversely, inclusion of the 22 bp cassette exon or both the 18 and 22 bp cassette exons decreased with cancer stage (Fig. 6B). Indeed, studies have linked RPS24 splicing with the incidence of several cancers without selecting hypoxia as a specific parameter (Danan-Gotthold et al. 2015; Zhang et al. 2015; Munkley et al. 2019). In prostate cancer, the ESRP2 splicing factor represses the inclusion of the 22 bp cassette exon of RPS24 and was induced upon androgen stimulation (Munkley et al. 2019). It would be interesting to investigate whether hypoxia regulates ESRP2 or whether there are hypoxia-regulated splicing factors such as SRSF3 (Brady et al. 2017) that function on RPS24. In the human tumor samples that we acquired, hypoxia did not correlate with stage. In contrast to cell lines and spheroids, tumors are heterogeneous not only in oxygenation but cell type, so a reduced effect was expected. Since most of the hypoxic prostate tumors were in stage II, the RPS24 long variant could be a hypoxic biomarker for early stage detection although further investigation on a broader scale would be necessary.

In summary, we show that hypoxia influences the polysome association of select RPs and the alternative splicing of select RP mRNAs. Further examination of these changes in cells cultured under physiologically relevant oxygen conditions (physioxia) would be a valuable research avenue (Keeley and Mann 2019). Indeed, this emerging field will surely progress in the context of human biology to gain a greater appreciation that ribosome composition is heterogeneous in response to stressors in normal physiology and disease.

MATERIALS AND METHODS

Cell culture

All cell lines were used within 6 mo of being obtained from the American Type Culture Collection and maintained as suggested. Cells were incubated at 37°C in 5% CO_2 and either 21% O_2 (normoxia) or 1% O_2 (hypoxia) in a HypOxystation H35 for 24 h. Spheroids were generated by seeding 50,000 cells into round bottom, low-attachment 96-well plates (Corning) followed by gentle swirling to promote cell–cell contacts and incubated for 5 d. Hypoxia was confirmed via *SLC2A1* transcription induction.

Polysome isolation

Cell lysis, polysome fractionation and analysis, and protein isolation were performed as previously described (Timpano and Uniacke 2016). Polysomes were dissociated by adding 20 mM EDTA pH 8.0 to lysis buffer and sucrose gradients in the absence of cycloheximide.

TMT-mass spectrometry

Polysome fractions were pooled into monosome (M; single ribosomes), light polysomes (L; 2–4 ribosomes/mRNA), and heavy polysomes (H; ≥5 ribosomes/mRNA) prior to protein isolation. Protein abundances in L and H were made relative to M in normoxia and hypoxia. Mass spectrometry analyses were carried out in three biological replicates. TCA-precipitated proteins were reduced, alkylated, and digested with Trypsin/Lys-C, followed by labeling with TMT-10plex (ThermoFisher). Detailed protocol in Supplemental Information.

Transfection, RNA isolation, and RT-PCR or RT-qPCR

Cells (5×10^6) were seeded into 150 mm plates and transiently transfected (15 µg DNA) 24 h later using polyethylenimine (26 µg/mL final concentration) with either the empty plasmid control (pMyc-N1 was a gift from Lei Lu [Addgene plasmid # 85759;

http://n2t.net/addgene:85759; RRID:Addgene_85759]) or RPS12 (Myc-DDK carboxy-terminal tagged) Human Tagged ORF clone (Origene RC214733). Cells were lysed 48 h post-transfection and polysome fractionation and RNA isolation was performed as described previously (Timpano and Uniacke 2016). Reverse transcription was optimized for structured transcripts (Fig. 2A) by incubating equal volumes of RNA with random primers for 5 min at 65°C, followed by incubation on ice before adding the remaining kit components (Applied Biosystem High Capacity cDNA). End-point PCR was performed and band intensity was measured using Image Lab (BioRad), and the % mRNA was calculated for each fraction on the gradient out of the total band intensity from all fractions (Figs. 2A, 5A). For total mRNA abundance measurements on whole cell lysates (Figs. 2B, 6B), cells were lysed using RiboZol (VWR) according to the manufacturer's protocol. Reverse transcription of 2 µg of RNA was performed as per manufacturer's instructions (Applied Biosystem High Capacity cDNA). Quantitative PCR was performed using SsoAdvanced Universal SYBR Green Supermix (BioRad). See Supplemental Table S1 for primer sequences.

RNA isolation for ASPCR

Cells were lysed using RiboZol (VWR) according to the manufacturer's protocol. RNA was purified using PureLink RNA Mini Kit (Life Technologies) with on-column DNase I treatment (BioBasic). RNA integrity confirmed using Agilent Bioanalyzer prior to reverse transcription. ASPCR was performed as described previously to quantify 68 ASEs within RP mRNAs (Klinck et al. 2008). Briefly, end-point PCR using primers flanking splicing events (see Supplemental Table S1 for primer sequences) was followed by capillary electrophoresis to separate and quantify amplicons. Using the most predominant splicing event, the PSI was calculated as the ratio of long amplicon over the sum of short and long amplicons. Splicing of *RPS24* in prostate tumors was measured using Origene TissueScan prostate tumor cDNA panels II and III (normalized to β-Actin) and the C_t value of *CAIX* was used to measure the degree of hypoxia.

Western blotting

Standard western blotting procedure was used. Primary antibodies (all antibodies diluted at 1/1000, except for β-Actin at 1/20,000): anti-FLAG (F1804; Sigma), anti-β-Actin (GT5512; GeneTex), anti-RPS24 (A303-842A; Bethyl), anti-RPS12 (ab175219; Abcam), anti-RPL5 (ab137617; Abcam), anti-p53 (sc-126; Santa Cruz), and anti-c-Myc (sc-40, Santa Cruz). Secondary antibodies diluted at 1/5000 were HRP-conjugated anti-rabbit and anti-mouse (Promega). Densitometry was performed using Image Lab (BioRad).

Generation of stable FLAG-RPS24 cell lines

PCR-based cloning was used to insert the coding sequence of the RPS24 short or long variant into p3XFLAG-CMV-10puroE- with amino-terminal tag. Stable cell lines were generated in U87MG by transfection with Lipofectamine 2000 (Invitrogen) and selection in 1 µg/mL puromycin to generate stable single clones.

Statistical analyses

All statistical analyses were performed using GraphPad Prism 7.0. Experimental data were tested using unpaired two-tailed Student's *t*-test when only two means were compared, or a one-way ANOVA followed by Tukey's HSD test when three or more means were compared. $P < 0.05$ was considered statistically significant. Prostate tumor samples were analyzed by correlating *CAIX* C_t value with PSI using Spearman's correlation coefficient. Tumor stage and PSI were compared using Kruskal–Wallis test (one-way ANOVA) followed by Dunn's multiple comparisons test.

SUPPLEMENTAL MATERIAL

Supplemental material is available for this article.

ACKNOWLEDGMENTS

We thank Mathieu Durand and Philippe Thibault at Université de Sherbrooke Rnomics Platform (http://rnomics.med.usherbrooke.ca) for ASPCR service, Jonathan Krieger at SPARC BioCentre at The Hospital for Sick Children for TMT service, Kari Dunfield for use of the iQ5 PCR system, and Lorian Fay and Michael Rosen for technical support. This work was funded by the Natural Sciences and Engineering Council of Canada grant number 04807 and the Canadian Institutes of Health Research (PJT 152925) to J.U. A.B. was supported by a Natural Sciences and Engineering Council of Canada Alexander Graham Bell Canada Graduate Scholarship.

Received January 8, 2019; accepted January 2, 2020.

REFERENCES

Andreev DE, Dmitriev SE, Zinovkin R, Terenin IM, Shatsky IN. 2012. The 5′ untranslated region of Apaf-1 mRNA directs translation under apoptosis conditions via a 5′ end-dependent scanning mechanism. *FEBS Lett* **586:** 4139–4143. doi:10.1016/j.febslet.2012.10.010

Anger AM, Armache JP, Berninghausen O, Habeck M, Subklewe M, Wilson DN, Beckmann R. 2013. Structures of the human and *Drosophila* 80S ribosome. *Nature* **497:** 80–85. doi:10.1038/nature12104

Bhat M, Robichaud N, Hulea L, Sonenberg N, Pelletier J, Topisirovic I. 2015. Targeting the translation machinery in cancer. *Nat Rev Drug Discov* **14:** 261–278. doi:10.1038/nrd4505

Brady LK, Wang H, Radens CM, Bi Y, Radovich M, Maity A, Ivan C, Ivan M, Barash Y, Koumenis C. 2017. Transcriptome analysis of hypoxic cancer cells uncovers intron retention in EIF2B5 as a mechanism to inhibit translation. *PLoS Biol* **15:** e2002623. doi:10.1371/journal.pbio.2002623

Bryant JD, Brown MC, Dobrikov MI, Dobrikova EY, Gemberling SL, Zhang Q, Gromeier M. 2018. Regulation of hypoxia-inducible factor 1α during hypoxia by DAP5-induced translation of PHD2. *Mol Cell Biol* **38**. doi:10.1128/MCB.00647-17

Chaudhuri S, Vyas K, Kapasi P, Komar AA, Dinman JD, Barik S, Mazumder B. 2007. Human ribosomal protein L13a is dispensable for canonical ribosome function but indispensable for efficient rRNA methylation. *RNA* **13:** 2224–2237. doi:10.1261/rna.694007

Coldwell MJ, Mitchell SA, Stoneley M, MacFarlane M, Willis AE. 2000. Initiation of Apaf-1 translation by internal ribosome entry. *Oncogene* **19:** 899–905. doi:10.1038/sj.onc.1203407

Coudert L, Adjibade P, Mazroui R. 2014. Analysis of translation initiation during stress conditions by polysome profiling. *J Vis Exp*. doi:10.3791/51164

Danan-Gotthold M, Golan-Gerstl R, Eisenberg E, Meir K, Karni R, Levanon EY. 2015. Identification of recurrent regulated alternative splicing events across human solid tumors. *Nucleic Acids Res* **43:** 5130–5144. doi:10.1093/nar/gkv210

Ferretti MB, Ghalei H, Ward EA, Potts EL, Karbstein K. 2017. Rps26 directs mRNA-specific translation by recognition of Kozak sequence elements. *Nat Struct Mol Biol* **24:** 700–707. doi:10.1038/nsmb.3442

Gupta V, Warner JR. 2014. Ribosome-omics of the human ribosome. *RNA* **20:** 1004–1013. doi:10.1261/rna.043653.113

Hashem Y, des Georges A, Dhote V, Langlois R, Liao HY, Grassucci RA, Hellen CU, Pestova TV, Frank J. 2013. Structure of the mammalian ribosomal 43S preinitiation complex bound to the scanning factor DHX29. *Cell* **153:** 1108–1119. doi:10.1016/j.cell.2013.04.036

Ho JJD, Wang M, Audas TE, Kwon D, Carlsson SK, Timpano S, Evagelou SL, Brothers S, Gonzalgo ML, Krieger JR, et al. 2016. Systemic reprogramming of translation efficiencies on oxygen stimulus. *Cell Rep* **14:** 1293–1300. doi:10.1016/j.celrep.2016.01.036

Ho JJD, Balukoff NC, Cervantes G, Malcolm PD, Krieger JR, Lee S. 2018. Oxygen-sensitive remodeling of central carbon metabolism by archaic eIF5B. *Cell Rep* **22:** 17–26. doi:10.1016/j.celrep.2017.12.031

Hockel M, Schlenger K, Aral B, Mitze M, Schaffer U, Vaupel P. 1996. Association between tumor hypoxia and malignant progression in advanced cancer of the uterine cervix. *Cancer Res* **56:** 4509–4515.

Holcik M, Sonenberg N. 2005. Translational control in stress and apoptosis. *Nat Rev Mol Cell Biol* **6:** 318–327. doi:10.1038/nrm1618

Keeley TP, Mann GE. 2019. Defining physiological normoxia for improved translation of cell physiology to animal models and humans. *Physiol Rev* **99:** 161–234. doi:10.1152/physrev.00041.2017

Khatter H, Myasnikov AG, Natchiar SK, Klaholz BP. 2015. Structure of the human 80S ribosome. *Nature* **520:** 640–645. doi:10.1038/nature14427

Klinck R, Bramard A, Inkel L, Dufresne-Martin G, Gervais-Bird J, Madden R, Paquet ER, Koh C, Venables JP, Prinos P, et al. 2008. Multiple alternative splicing markers for ovarian cancer. *Cancer Res* **68:** 657–663. doi:10.1158/0008-5472.CAN-07-2580

Kondrashov N, Pusic A, Stumpf CR, Shimizu K, Hsieh AC, Xue S, Ishijima J, Shiroishi T, Barna M. 2011. Ribosome-mediated specificity in Hox mRNA translation and vertebrate tissue patterning. *Cell* **145:** 383–397. doi:10.1016/j.cell.2011.03.028

Kurylo CM, Parks MM, Juette MF, Zinshteyn B, Altman RB, Thibado JK, Vincent CT, Blanchard SC. 2018. Endogenous rRNA sequence variation can regulate stress response gene expression and phenotype. *Cell Rep* **25:** 236–248.e236. doi:10.1016/j.celrep.2018.08.093

Lacerda R, Menezes J, Romão L. 2017. More than just scanning: the importance of cap-independent mRNA translation initiation for cellular stress response and cancer. *Cell Mol Life Sci* **74:** 1659–1680. doi:10.1007/s00018-016-2428-2

Liu B, Qian SB. 2014. Translational reprogramming in cellular stress response. *Wiley Interdiscip Rev RNA* **5:** 301–315. doi:10.1002/wrna.1212

Liu L, Simon MC. 2004. Regulation of transcription and translation by hypoxia. *Cancer Biol Ther* **3:** 492–497. doi:10.4161/cbt.3.6.1010

Lyabin DN, Ovchinnikov LP. 2016. Selective regulation of YB-1 mRNA translation by the mTOR signaling pathway is not mediated by 4E-binding protein. *Sci Rep* **6:** 22502. doi:10.1038/srep22502

Munkley J, Li L, Krishnan SRG, Hysenaj G, Scott E, Dalgliesh C, Oo HZ, Maia TM, Cheung K, Ehrmann I, et al. 2019. Androgen-regulated transcription of ESRP2 drives alternative splicing patterns in prostate cancer. *Elife* **8**. doi:10.7554/eLife.47678

O'Donohue MF, Choesmel V, Faubladier M, Fichant G, Gleizes PE. 2010. Functional dichotomy of ribosomal proteins during the synthesis of mammalian 40S ribosomal subunits. *J Cell Biol* **190:** 853–866. doi:10.1083/jcb.201005117

Padrón A, Iwasaki S, Ingolia NT. 2019. Proximity RNA labeling by APEX-seq reveals the organization of translation initiation complexes and repressive RNA granules. *Mol Cell* **75:** 875–887.e875. doi:10.1016/j.molcel.2019.07.030

Parsyan A, Shahbazian D, Martineau Y, Petroulakis E, Alain T, Larsson O, Mathonnet G, Tettweiler G, Hellen CU, Pestova TV, et al. 2009. The helicase protein DHX29 promotes translation initiation, cell proliferation, and tumorigenesis. *Proc Natl Acad Sci* **106:** 22217–22222. doi:10.1073/pnas.0909773106

Pisareva VP, Pisarev AV. 2016. DHX29 and eIF3 cooperate in ribosomal scanning on structured mRNAs during translation initiation. *RNA* **22:** 1859–1870. doi:10.1261/rna.057851.116

Rabl J, Leibundgut M, Ataide SF, Haag A, Ban N. 2011. Crystal structure of the eukaryotic 40S ribosomal subunit in complex with initiation factor 1. *Science* **331:** 730–736. doi:10.1126/science.1198308

Robledo S, Idol RA, Crimmins DL, Ladenson JH, Mason PJ, Bessler M. 2008. The role of human ribosomal proteins in the maturation of rRNA and ribosome production. *RNA* **14:** 1918–1929. doi:10.1261/rna.1132008

Robles AI, Bemmels NA, Foraker AB, Harris CC. 2001. APAF-1 is a transcriptional target of p53 in DNA damage-induced apoptosis. *Cancer Res* **61:** 6660–6664.

Semenza GL. 2012. Hypoxia-inducible factors in physiology and medicine. *Cell* **148:** 399–408. doi:10.1016/j.cell.2012.01.021

Shi Z, Fujii K, Kovary KM, Genuth NR, Röst HL, Teruel MN, Barna M. 2017. Heterogeneous ribosomes preferentially translate distinct subpools of mRNAs genome-wide. *Mol Cell* **67:** 71–83.e77. doi:10.1016/j.molcel.2017.05.021

Slavov N, Semrau S, Airoldi E, Budnik B, van Oudenaarden A. 2015. Differential stoichiometry among core ribosomal proteins. *Cell Rep* **13:** 865–873. doi:10.1016/j.celrep.2015.09.056

Timpano S, Uniacke J. 2016. Human cells cultured under physiological oxygen utilize two cap-binding proteins to recruit distinct mRNAs for translation. *J Biol Chem* **291:** 10772–10782. doi:10.1074/jbc.M116.717363

Uniacke J, Holterman CE, Lachance G, Franovic A, Jacob MD, Fabian MR, Payette J, Holcik M, Pause A, Lee S. 2012. An oxygen-regulated switch in the protein synthesis machinery. *Nature* **486:** 126–129. doi:10.1038/nature11055

van de Waterbeemd M, Tamara S, Fort KL, Damoc E, Franc V, Bieri P, Itten M, Makarov A, Ban N, Heck AJR. 2018. Dissecting ribosomal particles throughout the kingdoms of life using advanced hybrid mass spectrometry methods. *Nat Commun* **9:** 2493. doi:10.1038/s41467-018-04853-x

Xue S, Tian S, Fujii K, Kladwang W, Das R, Barna M. 2015. RNA regulons in Hox 5′ UTRs confer ribosome specificity to gene regulation. *Nature* **517:** 33–38. doi:10.1038/nature14010

Zhang Y, Lu H. 2009. Signaling to p53: ribosomal proteins find their way. *Cancer Cell* **16:** 369–377. doi:10.1016/j.ccr.2009.09.024

Zhang H, Ye J, Weng X, Liu F, He L, Zhou D, Liu Y. 2015. Comparative transcriptome analysis reveals that the extracellular matrix receptor interaction contributes to the venous metastases of hepatocellular carcinoma. *Cancer Genet* **208:** 482–491. doi:10.1016/j.cancergen.2015.06.002